

This is a postprint version of the following published document:

Gómez, M., Castejón, C. & García-Prada, J. (2016). Automatic condition monitoring system for crack detection in rotating machinery. *Reliability Engineering & System Safety*, vol. 152, pp. 239–247.

DOI: [10.1016/j.ress.2016.03.013](https://doi.org/10.1016/j.ress.2016.03.013)

© 2016 Elsevier Ltd.

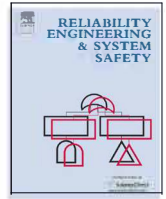


This work is licensed under a [Creative Commons Attribution-NonCommercial-NoDerivatives 4.0 International License](https://creativecommons.org/licenses/by-nc-nd/4.0/).



Contents lists available at ScienceDirect

Reliability Engineering and System Safety

journal homepage: www.elsevier.com/locate/ress

Automatic condition monitoring system for crack detection in rotating machinery

M.J. Gómez*, C. Castejón, J.C. García-Prada

MAQLAB Group, Mechanical Department, University Carlos III of Madrid, Av. de la Universidad, 30, 28911, Leganés, Madrid, Spain

ARTICLE INFO

Article history:

Received 1 January 2016

Received in revised form

15 March 2016

Accepted 22 March 2016

Keywords:

Cracked shaft detection

Wavelet transform

Intelligent Classification Systems

Condition monitoring

Artificial Neural Networks

ABSTRACT

Maintenance is essential to prevent catastrophic failures in rotating machinery. A crack can cause a failure with costly processes of repair, especially in a rotating shaft.

In this study, the Wavelet Packets transform energy combined with Artificial Neural Networks with Radial Basis Function architecture (RBF-ANN) are applied to vibration signals to detect cracks in a rotating shaft. Data were obtained from a rig where the shaft rotates under its own weight, at steady state at different crack conditions. Nine defect conditions were induced in the shaft (with depths from 4% to 50% of the shaft diameter). The parameters for Wavelet Packets transform and RBF-ANN are selected to optimize its success rates results. Moreover, 'Probability of Detection' curves were calculated showing probabilities of detection close to 100% of the cases tested from the smallest crack size with a 1.77% of false alarms.

© 2016 Published by Elsevier Ltd.

1. Introduction

The main objective of condition monitoring of rotating machinery is to detect faults before a catastrophic failure occurs. Besides, detection must arrive early enough to have time for programming a stop at the most convenient moment. This kind of maintenance has a lot of advantages, such as the avoidance of stopping and dismount the elements of the machine to check its status, and the increasing of probability of fault detection. Condition monitoring improves safety and costs of processes, reason why it has focused a lot of attention in lasts decades.

In an industrial process, when a defect is detected, three main stages are passed through; the first one is detection, the second one is diagnosis and the third one is intervention to correct undesired effects. Condition monitoring is usually based on the control of certain parameter that is considered fault indicator, and when its value exceed certain limits it is considered that a fault exists. Nowadays, vibration analysis is the most extended technique for condition monitoring [1].

A vibration signal obtained from a rotating machine has a complex structure and comprises a high number of data. The key of the process is the feature extraction. Feature extraction consist on finding the proper processing for a vibration signal to get parameters easier to handle, and also representative of the real

status of the machine. Features must content reliable information about the fault.

After the features extraction, a classification system is needed to automate the diagnosis process. The classification system automatically decides the output of the system avoiding human factors. The process of this type of methods is schemed in Fig. 1

Many fault diagnosis algorithms have been proposed both for features extraction and for classification.

Regarding feature extraction, several approaches have been used for signal analysis. Fourier theory (FT) and techniques derived from it, as Fast Fourier transform (FFT) and Hilbert transform (HT), have traditionally been used to observe changes in the response when a fault appears [2,3]. However, FT and most techniques derived from it are inappropriate to treat non stationary signals, that are commonly obtained from rotating machinery, due to the absence of temporary information. The short time Fourier transform (STFT) is suitable to treat nonstationary signals, however its main disadvantage is that the frequency resolution obtained is constant for the whole signal, since the window applied is the same. Therefore, new techniques working both in time and in frequency domain have appeared, such as Hilbert–Huang Transform (HHT) [4] and Wavelet Transform (WT) [5].

Specifically, WT is a especially effective tool in treating non-stationary signals and has become one of the most widely used techniques for signal processing. Currently, applications of the WT are increasing, and they are now used for speech recognition [6,7]; denoising [8]; electrocardiographs [9]; and diagnosis of cracked

* Corresponding author.

E-mail address: mjggarci@ing.uc3m.es (M.J. Gómez).

rotating elements [10] as bearings [11], gears [12], and beams [13,14].

Regarding classification systems, these include artificial neural networks (ANN), fuzzy logic (FL), genetic algorithms (GA), bayesian classifier (BC) and support vector machines (SVM), among others. Specifically ANNs have been widely used for different applications, such as residual life estimation of mechanical elements [15], degradation prediction [16], diagnose accident scenarios as in [17] or [18], diagnosis of cracked shafts detection [19,20].

The main advantage of ANNs is their flexibility and capability of learning complex nonlinear relationships between input and output. The critical stage for ANNs is to choose the training parameters used to learn the structure of the problem [21]. On the other hand, the main drawback of the use of ANNs is the need of a large amount of historical data, not only extracted from healthy condition, but also from faulty condition, to facilitate the proper training of the system [22].

Fault detection is specially critical for shafts, due to the high loads they support. The dynamical behavior of a cracked rotor has focused a lot of interest among researchers [23–26]. A crack in a shaft can cause a failure with costly processes of reparation. Cracked shaft detection has used combination of WT and ANN for signals coming from models in cases such as [27,28].

The present work details an integrated system for maintenance based on the combination of energy features and a trained ANN. The feature extraction is calculated from a vibration signal by means of the Wavelet Packets Transform (WPT). The technique is applied to experimental signals, showing that the reliability of the technique is high.



Fig. 1. Scheme of current processes of condition monitoring.

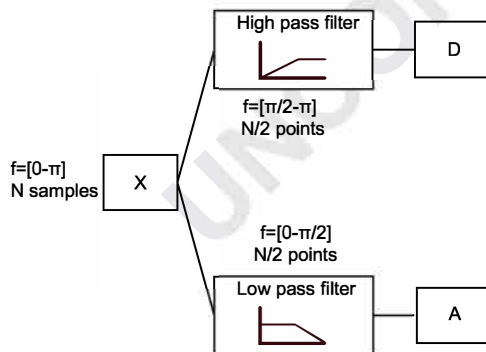


Fig. 2. DWT decomposition of a signal (S) in approximation information (A) and detail information (D) using filters.

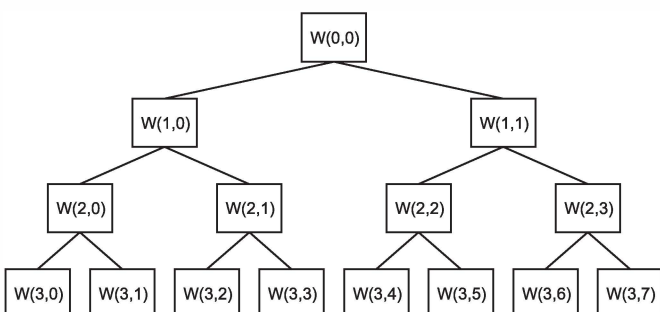


Fig. 3. WPT decomposition process until decomposition level 3.

2. Wavelet packets transform

The WT is especially efficient at performing local analysis of non-stationary signals. The discrete wavelet transform (DWT) is more commonly used than the continuous form of the WT because signals usually comprise discrete data and the computational cost is lower. Following Mallat definitions [29], the DWT can be implemented using filters. The signal is decomposed being passed through a low-pass filter g to obtain the wavelet approximation (A), and a high pass filter h to obtain the wavelet detail (D), as in Fig. 2. DWT decomposition halves the frequency band of the input; thus, following the Nyquist rule, it is justified to down-sample by two [30].

Several types of analysis are performed by the recursive application of the DWT, such as Multiresolution Analysis (MRA) and Wavelet Packets Transform (WPT). The wavelet packets transform (WPT) was used to prevent problems associated to MRA, where the downsampling process can only be performed for the A information. WPT allows A and D information to be decomposed recursively until the desired resolution, as shown in Fig. 3.

$W(k,j)$ represents coefficients of the signal in each packet, k represents the decomposition level, and j represents the position of the packet within the decomposition level. Each correlation vector $W(k,j)$ has the structure:

$$W(k,j) = \{w_1(k,j), \dots, w_N(k,j)\} = \{w_i(k,j)\} \quad (1)$$

The calculus of energy using WPT is similar to the used in the FFT [5]. The energy of a certain packet j within the

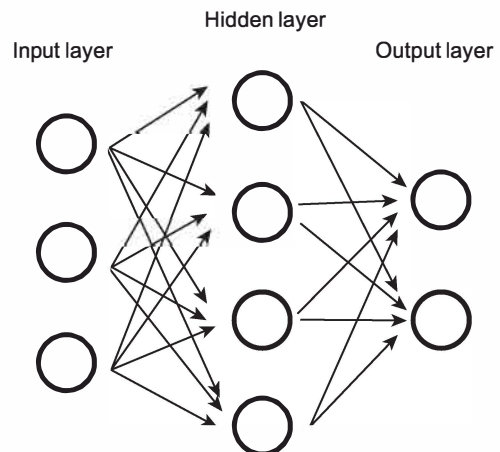


Fig. 4. ANN basic structure.



Fig. 5. Rig used for experimental setup.

decomposition level k can be obtained as the sum of the squares of its coefficients,

$$E_{kj} = \sum_i \{w_i(k, j)\}^2 \quad (2)$$

3. ANN classification systems

Currently, ANNs focus great interest both at academic and industrial level [31]. ANNs are an example of learning and automatic processing inspired in the way that the human nervous system works. It comprises an interconnecting system of neurons that collaborate to produce an output. ANNs are widely used as an effective, cost-effective and efficient automated indicator of health of modern engineering systems [32].

There are two main phases in the use of an ANN; the phase of learning or training, and the phase of validation and use. For the most common case of supervised learning, the stage of training consists on the presentation of a set of input patterns, which output is known. The network adjusts the connections in an iterative process of error minimization, until it gets the admissible level of error. However, the accuracy of ANNs depends upon the features selected, ANN architecture, training parameters and training set size.

The radial basis function (RBF) architecture constitutes one of the more widely used ANN in the diagnosis of defects area [33]. It

was created with the main purpose of working on real time applications. The name of radial basis function derives from the fact that the function is symmetric; the output is the same for inputs that are at the same distance of the center.

RBF networks are constituted by at least three layers of neurons; one at the input, one hidden and one at the output, as shown in Fig. 4. These layers are characterized by having local character, each neuron activates in a different region of the space of the input patterns.

The use of RBF architecture offers a lot of advantages such as a fast training, and easy optimization due to the low number of design parameters [34]. The design parameters of an ANN-RBF are the activation function and the stopping criteria for the training. The most common used activation function is the Gaussian, thus the *spread* of the function must be selected. The most common stopping criteria is a goal sum-squared error (SSE) between the desired output and the real output. The ANN creates one neuron in the hidden layer at each iteration. When SSE falls beneath the goal error or a maximum number of neurons (to be selected) has been reached the training stops.

4. Experimental setup

The experimental measurements are obtained from a machine simulation fault created by *SpectraQuest*[®] that can be observed in Fig. 5.

The rig comprises a motor *Marathon*[®], with maximum speed of 10,000 r.p.m. and a power of 0.75 kW, that drives the shaft by means of an elastic coupling. The shaft rotates with the load of its own weight. The speed of the motor is set using a regulator *S1 Delta*[®] S1, and controlled using an optical tachometer *Banner*[®]. The shaft is supported by two ball bearings *ER10 Rexnord*[®].

The tested element is the shaft, under different crack conditions. A first test is made at healthy state, and then nine different crack levels (a) were induced by saw cuts. All the cracks were induced without dismounting the shaft from the machine, because usually cracks appear and grow while the machine rotates and the assembly effects are constant. The values of a in Table 1 are expressed as the ratio between the crack depth d and shaft diameter D , where $D=16$ mm.

Test are carried out at steady state at three different rotational speeds, shown in Table 2. Thus, 30 different conditions are tested; 10 different crack conditions and 3 rotation speeds.

For all cases, the cracks are located in the middle section, as shown in Fig. 6.

Table 1
Crack depths a used for the experimental setup, expressed in relative terms with respect to the diameter of the shaft D .

Defect level	0	1	2	3	4	5	6	7	8	9
Value ($a=d/D$)	0	0.04	0.08	0.12	0.17	0.22	0.28	0.33	0.42	0.5

Table 2
Rotational speeds used for the tests.

Speed	Value (Hz)
Speed 1	20
Speed 2	40
Speed 3	60

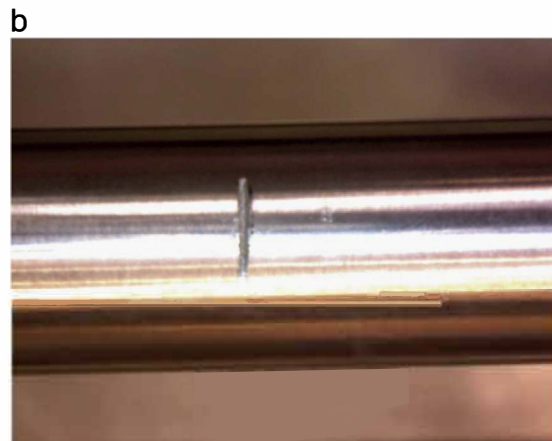
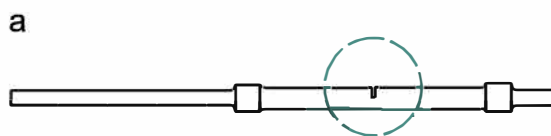


Fig. 6. Shaft and position of crack induced (a) and detail of an induced crack level 2.

Shaft properties were determined experimentally and are shown in Table 3.

The accelerometer used is 4374 B&K. The measurement direction is vertical and is mounted on the housing bearing. The accelerometer is connected to a signal conditioner B&K NEXUS, and to an acquisition card Keithley KUSB-100. The acquisition card is connected to a computer with the software called Btool, that was specifically designed for this purpose in Matlab® [35]. The measurement chain can be observed in Fig. 7.

The characteristics of the signals measured and number of signals are shown in Table 4.

5. Results and discussion

First, the features extraction stage is carried out by means of WPT energy. Later, several ANNs are trained trying to optimize their parameters to maximize success rates and minimize computational cost.

5.1. Feature extraction and selection using WPT

The energy calculated using WPT is selected for feature extraction due to its proven effectiveness to process non-stationary signals for diagnosis purpose [36,34]. The WPT is not a straightforward issue since some parameters must be selected.

The first one is the wavelet function. In this study, the 'Daubechies 6' wavelet function was applied due to the goodness of the results in this area [27]. The other parameter to be selected is the decomposition level, which determines the frequency resolution offered by each packet (same for all packets). Using a decomposition level of k , the number of packets obtained is $P=2^k$. By considering the global frequency of the signals as half of the sampling frequency $f_s/2$ according to the Nyquist theorem, the frequency resolution f_r of each packet is [34]:

$$f_r = \frac{f_s/2}{2^k} \quad (3)$$

In this study, the selection of the decomposition level is performed according to the method proposed in [28]. The method determines the optimal the decomposition level that maximizes the success rates of an ANN. WPT energies from 2 ($P=4$ packets; $f_r = 1500$ Hz) to 9 ($P=512$ packets; $f_r = 5.86$ Hz) are evaluated in the present work. Features considered are single level.

After preliminary studies, it was concluded that using all the packets of a single level for decomposition levels from 6 to 9 the computational cost is high. Therefore, for decomposition levels

from 6 to 9, the packets that experiment higher changes of energy when a crack appears are selected. Mean values of the 1500 signals measured by each condition are obtained. For each case of speed, the mean value of the healthy condition is subtracted to the mean value of each crack condition. The 10 packets that show higher differences in absolute value for each crack size are selected, according to Fig. 8.

Since 9 crack levels are tested, a number of packets between 10 and 90 could be selected for each speed, depending on the number of packets that are coincident for different crack sizes.

An analysis of the frequencies that present higher changes of energy with the crack is performed in [37], and they seem to be related to structural frequencies of the shaft.

Thus, input packets for the ANNs training are selected according to Table 5.

5.2. ANNs trained

Once the features are extracted and selected, the ANNs training is designed. Each energy of the packets selected represents one neuron in the input layer, thus the number of input neurons depends on the decomposition level.

The design parameters are selected according to preliminary studies. The number of neurons at the output layer is the number of possible answers of the ANN. In this case, ANNs did not offer good results when trying to determine the crack size, and the best results were obtained when 2 outputs are used: healthy or cracked.

When designing ANN, after the training stage a testing must come. Testing must use data not used for the training, so the number of data used for each stage must be selected. The values at the input and at the output must be normalized to increase stability of training and testing process [38].

The spread value of the Gaussian function will be selected to optimize the success rate of the ANN, thus an interval is proposed. Regarding the stopping criteria, a maximum value of SSE is proposed. If that value is not reached in a certain number of iterations or neurons in the hidden layer, that must also be selected, the training stops.

Table 6, show the common parameters selected for ANNs training, according to the inputs described in the previous section.

All parameters are selected to maximize the success rate number. To carry this, a total number of 456 ANNs were trained. From them, 24 optimal ANNs are selected, one by each decomposition level and speed.

Table 3
Shaft mechanical properties.

Mass (M) (kg)	0.378
Damping coefficient (c) (kg/s)	4.58
Stiffness (k) (KN/m)	1544.3
Rho (ρ) (m)	$2e-5$
Effective length (m)	0.26
Diameter (m)	0.0207

Table 4
Parameters of signals measured.

Parameter	Value
Sampling frequency f_s	6 kHz
Number of samples/signal	2^{14}
Number of signals/condition	1500

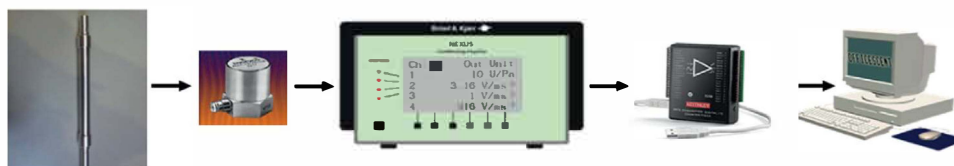


Fig. 7. Measurement chain.

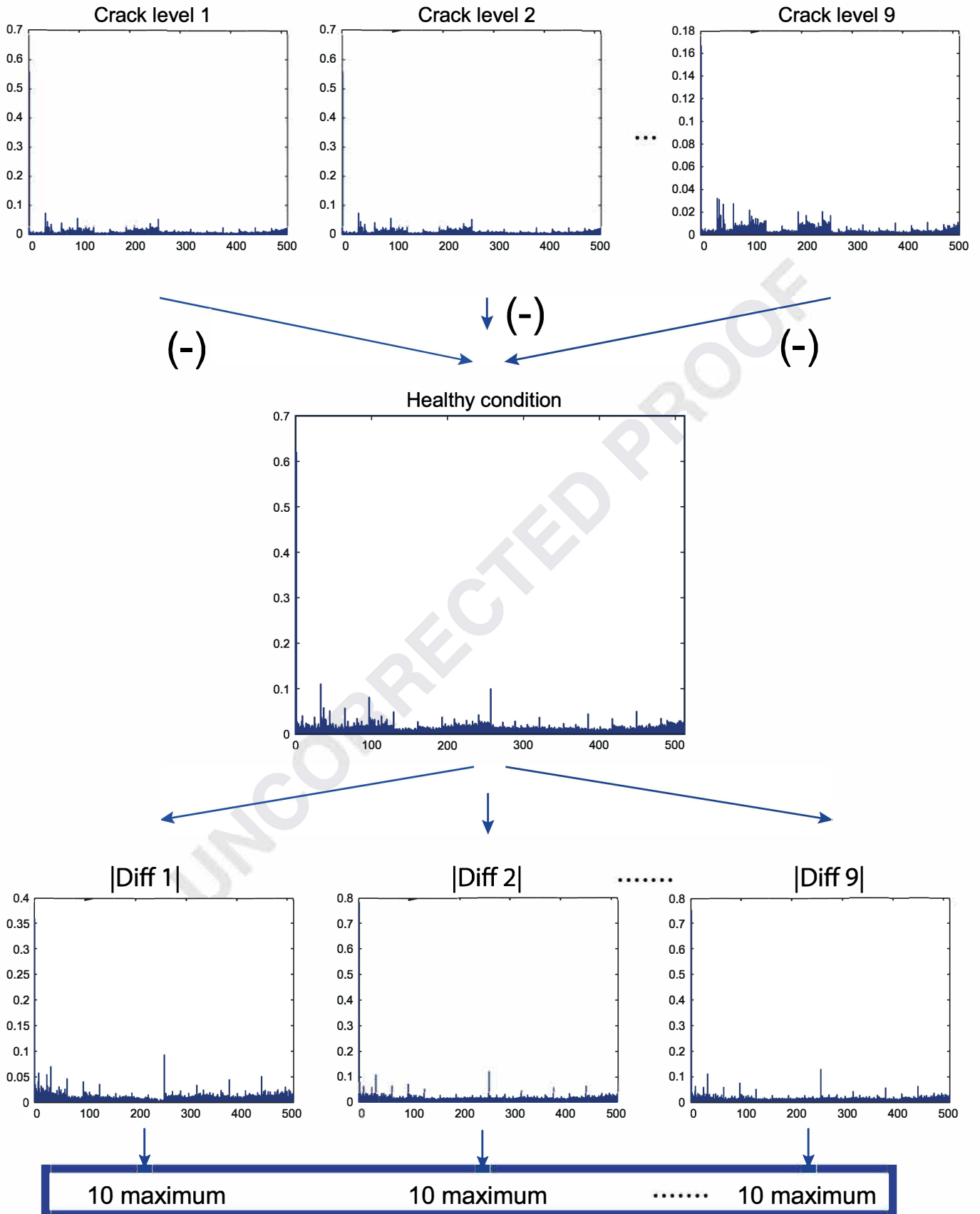


Fig. 8. Methodology for selecting significant packets for decomposition levels from 6 to 9.

5.3. Results

Results of the ANNs training are shown. For each speed, 8 optimal ANNs are selected, one for each decomposition level tested.

Table 5
Features selected for each decomposition level.

Decomposition level	Features selected
Low: from 2 to 5	All packets single level
High: from 6 to 9	10 maximum energy increments for each crack size

Table 6
Design parameters for ANN-RBF.

Normalization of input values	Between $[-1;1]$
Type of learning	Supervised
Number of neurons in output	2
Normalization of output values	$[-1,1]$
Input data distribution	Training 75%
	Test 25%
Stopping criteria	SSE 0.1–0.2
	Number of neurons at hidden layer 700
Spread	0.2–2

Fig. 9 presents success rates and number of neurons in the hidden layer of the 8 ANNs selected at 20 Hz, versus the decomposition level. It can be concluded that decomposition level 2 offers worst results than the rest, offering lower success rates and higher number of neurons. The results at other decomposition levels are similar.

Figs. 10 and 11 show results for 40 and 60 Hz respectively. For both cases, decomposition level number 5 seems to be the optimal one, and the speed of 60 Hz offers slightly better results.

ANNs training at decomposition level 2 always stops due to the maximum number of neurons in hidden layer neurons. Thus, the computational cost is higher and the success rate is lower than in other cases. For the rest of decomposition levels, the results are very similar at low and high decomposition levels at 20 Hz. On the other hand, at 40 and 60 Hz results at low decomposition levels (3, 4 and 5) show better results than at high decomposition levels (6, 7, 8 and 9).

5.4. POD calculation

The global success rate of an ANN gives important information about the diagnosis, however it is not accurate. There is a need to test the success of the ANN depending on the crack condition. There is a large difference if all the fails in the diagnosis of the ANN are accumulated in false alarms or in the crack level 1, that is not a critical crack.

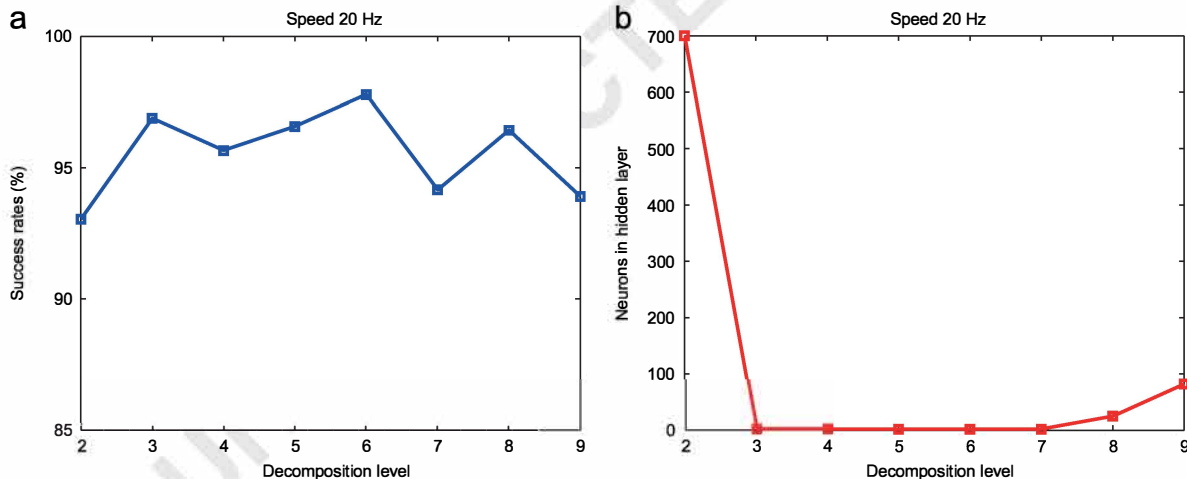


Fig. 9. Results of ANNs for each decomposition level at 20 Hz representing (a) success rates and (b) number of neurons in the hidden layer.

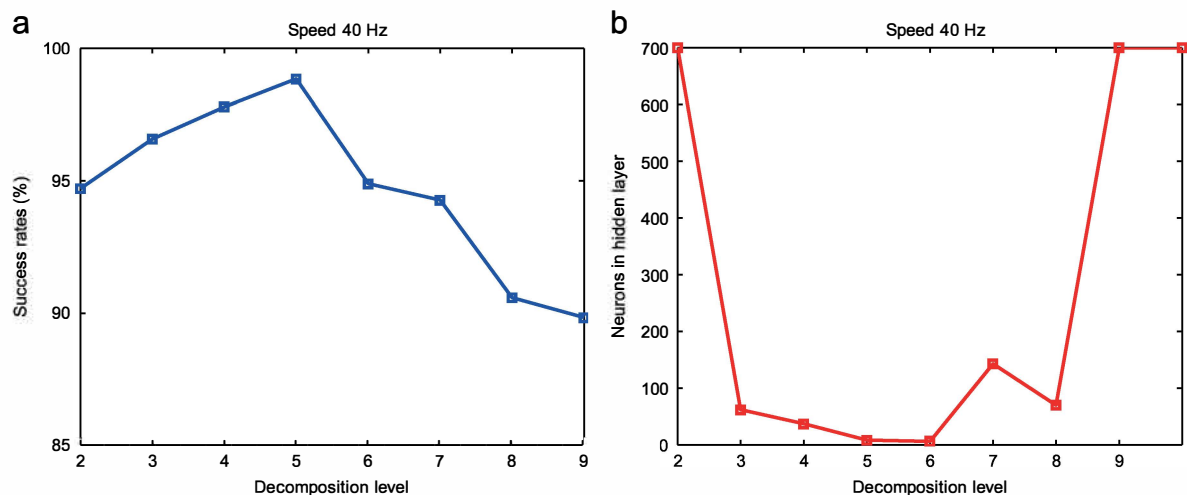


Fig. 10. Results of ANNs for each decomposition level at 40 Hz representing (a) success rates and (b) number of neurons in the hidden layer.

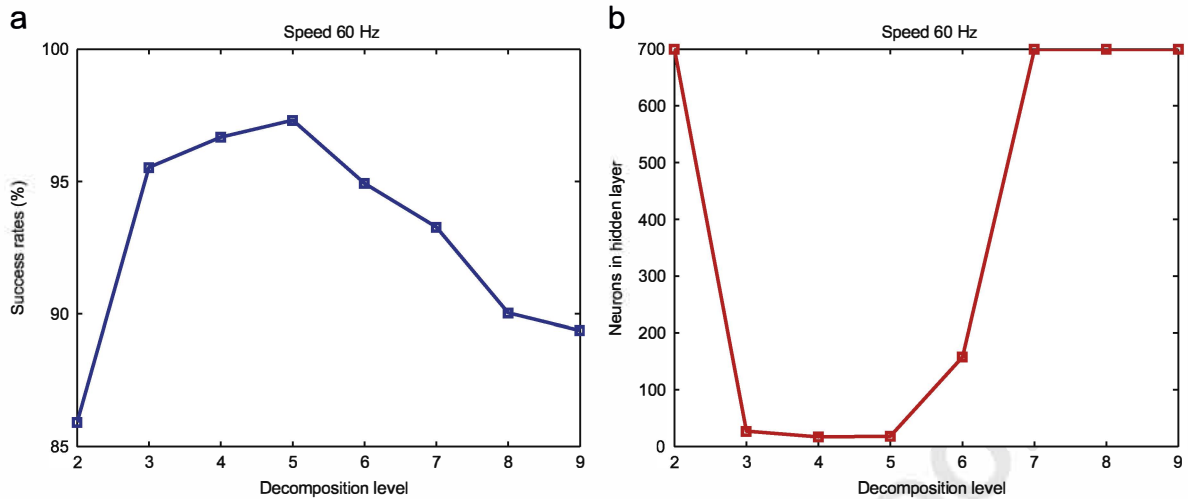


Fig. 11. Results of ANNs for each decomposition level at 60 Hz representing (a) success rates and (b) number of neurons in the hidden layer.

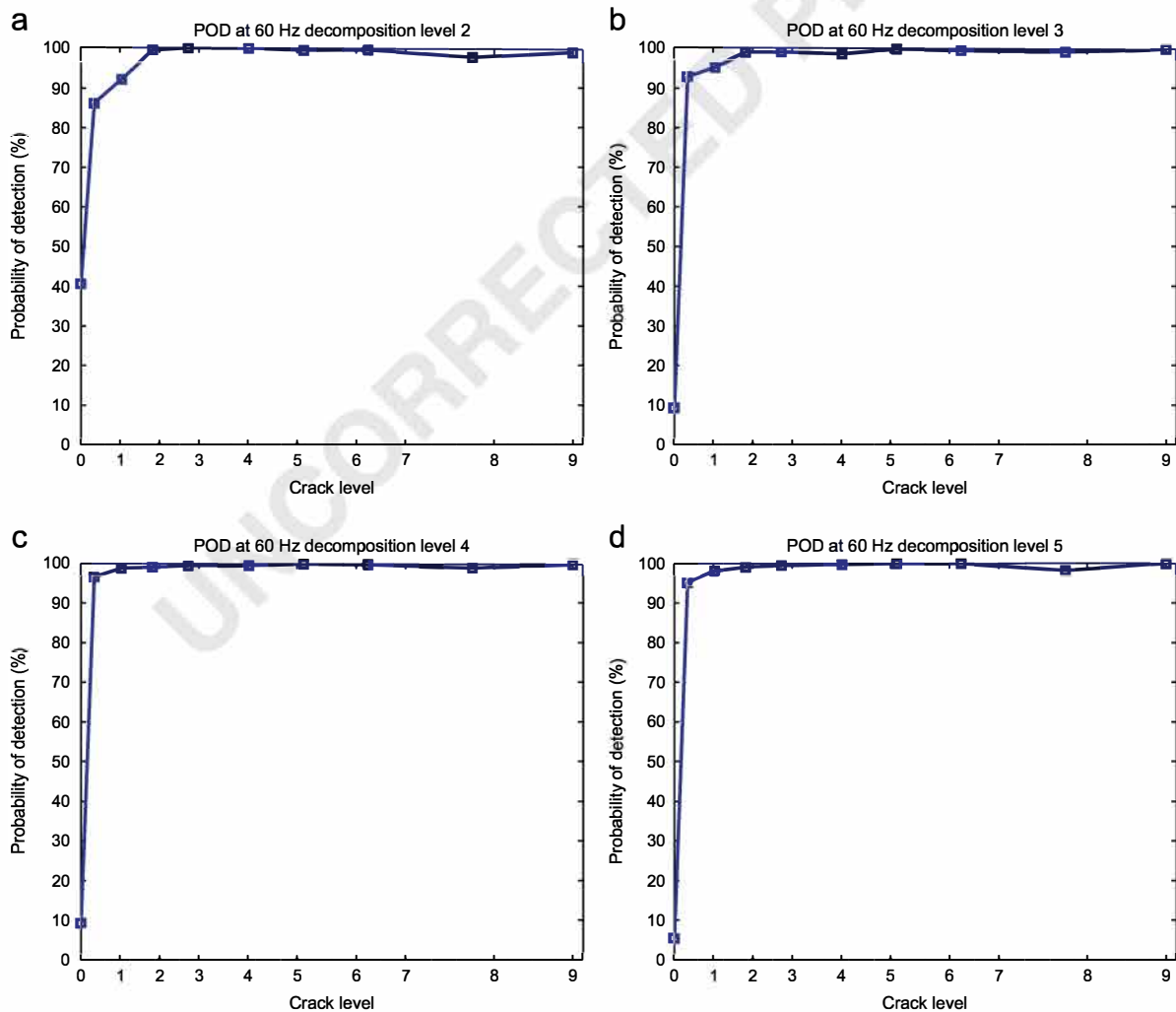


Fig. 12. POD curves obtained from ANNs at 60 Hz at low decomposition levels: (a) level 2, (b) level 3, (c) level 4, (d) level 5.

Thus, Probability of Detection (POD) curves are calculated using the results of success rates with the data kept for validation stage, for the three cases of speed. For all cases, decomposition level 5,

using all the energy packets obtained at that level, offers the best diagnosis results. Regarding the speed, the case of 60 Hz is the optimal one.

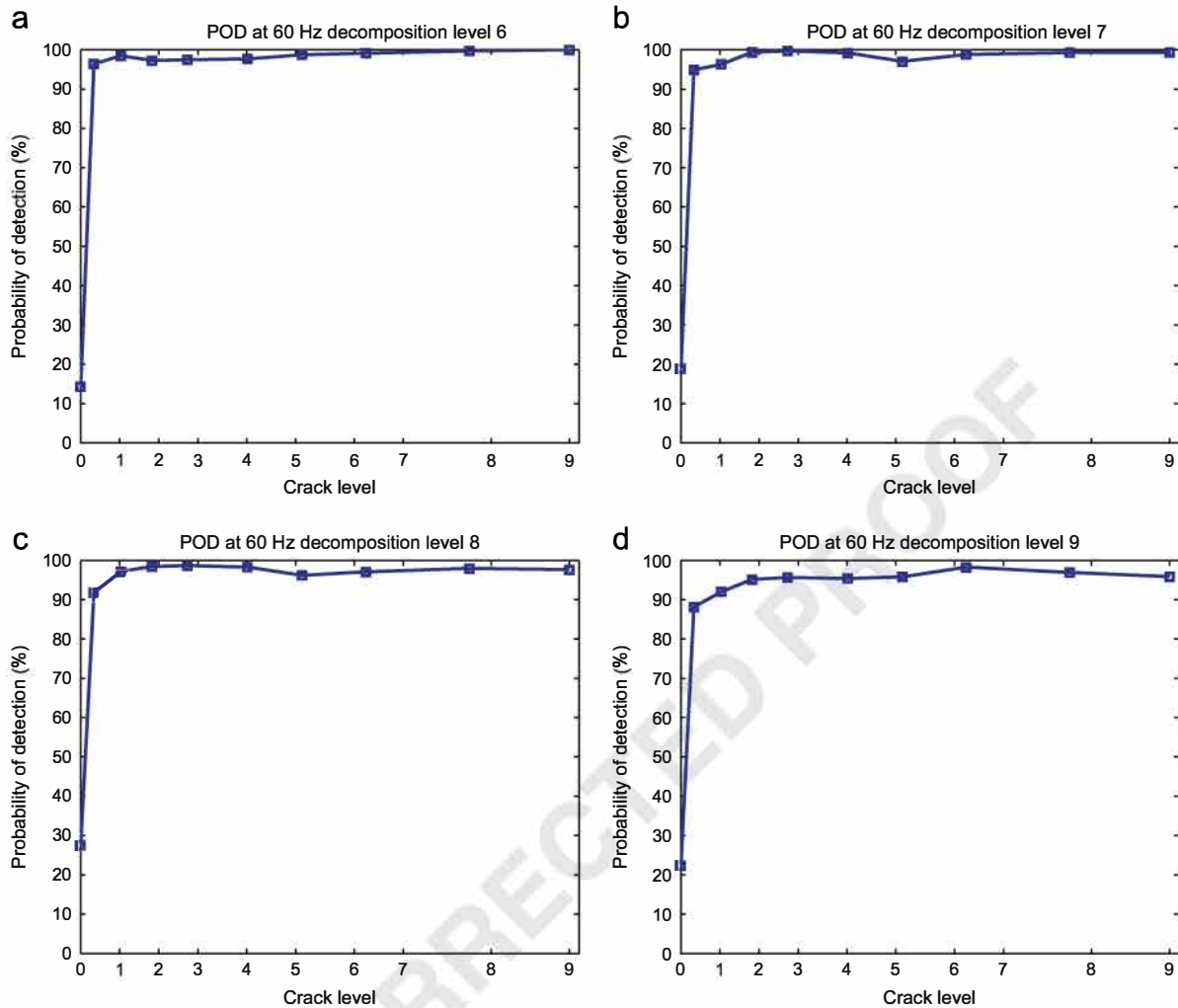


Fig. 13. POD curves obtained from ANNs at 60 Hz at high decomposition levels: (a) level 6, (b) level 7, (c) level 8, (d) level 9.

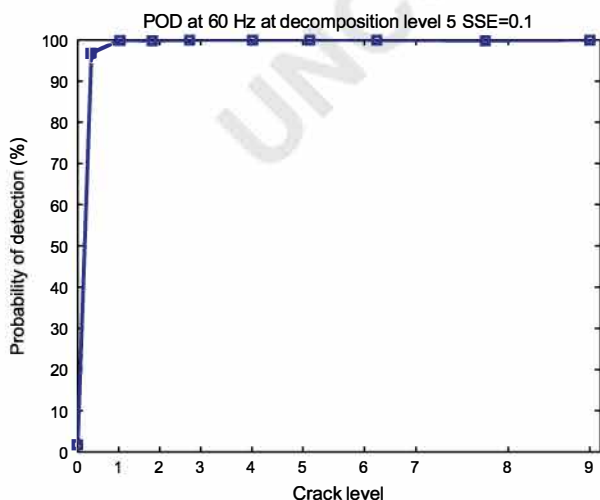


Fig. 14. POD at decomposition level 5 and goal 0.1 at 60 Hz.

POD curves at 60 Hz are shown in Figs. 12 and 13. The optimal decomposition level is number 5. High decomposition levels present a high number of false alarms.

Once the decomposition level 5–60 Hz is selected, a new ANN is trained using all the packets at this level with a $SSE=0.1$. Fig. 14

shows the POD curve calculated in this case. The ANN offers the best diagnosis results available with these data, with a number of false alarms of 1.77% and a low computational cost with only 45 neurons.

5.5. Discussion

The main contribution of the present work is the development of an expert system that is able to diagnose with reliability a crack in a rotating shaft using experimental vibration signals. The value of the work lies on the fact that most of the studies of the dynamical behavior of cracked rotors, specifically in shafts, do not involve the inverse process of crack detection and do not use experimental results [39].

Tests were carried out at different speeds that show that diagnosis results are improved with the speed. This can be assigned to the fact that when the speed increases, as the tests were performed at the same conditions, the signal-to-noise ratio is higher. Then, crack effects are more clearly distinguished when the speed increases.

The aim of the system proposed is to detect a crack when it appears and grows in a shaft, while it is rotating and thus, assembly influence is constant. The constant assembly influence has been reproduced in the present work tests, as the cracks are artificially induced in the shaft without dismounting it from the machine. Therefore, differences in signals measured are only

caused by crack effects and not by the assembly or other defects. In order to check if a mistuned assembly or other defects could hide the crack effects, and decrease the success rates obtained in this work, it would be necessary to make this specific tests, proposed as future work.

It would be interesting also to test if multi-level selection of WPT energies could improve the results in terms of success rates and computational cost. In this work the ANNs parameters and the decomposition level of the WPT are evaluated to optimize the success rates of the ANNs. However, all the energies selected are from the same level of decomposition (single-level).

6. Conclusions

For the present work, experimental vibration signals are taken from a rig at steady state at three different speeds and 10 different crack conditions (healthy and 9 crack levels from 4% of the shaft diameter to 50%). The signals are processed by means of WPT energy using 'Daubechies 6' as wavelet function. The single-level energies obtained are used to train several RBF-ANNs. The ANNs parameters and the decomposition level of the WPT are evaluated to optimize the success rates of the ANNs. Results seem to improve with the speed. Features extracted at decomposition level number 5 from signals obtained at the higher speed (60 Hz) offer the best results in terms of success rates and computational cost. Success rates are used to calculate POD curves and the number of false alarms is of 1.77% and crack levels above 1 can be detected with high reliability. Results show that the methodology proposed could be successfully integrated in industrial equipment for condition monitoring.

Acknowledgments

The authors would like to thank the Spanish Government for financing through the CDTI project RANKINE21 IDI-20101560.

References

- [1] Pedregal D, Carnero M. Vibration analysis diagnostics by continuous-time models: a case study. *Reliab Eng Syst Saf* 2009;94(2):244–53.
- [2] Sekhar A. On-line rotor fault identification by combined model and signal based approach. *Noise Vib Worldw* 2004;35(7):16–30.
- [3] Feldman M, Seibold S. Damage diagnosis of rotors: application of Hubert transform and multihypothesis testing. *J Vib Control* 1999;5(3):421–42.
- [4] Guo D, Peng Z. Vibration analysis of a cracked rotor using Hilbert–Huang transform. *Mech Syst Signal Process* 2007;21:3030–41.
- [5] Hu Q, He Z, Zhang Z, Zi Y. Fault diagnosis of rotating machinery based on improved wavelet package transform and svms ensemble. *Mech Syst Signal Process* 2007;21:668–705.
- [6] Vignolo L, Milone D, Rufiner H. Genetic wavelet packets for speech recognition. *Exp Syst Appl*.
- [7] Avci E, Akpolat ZH. Speech recognition using a wavelet packet adaptive network based fuzzy inference system. *Exp Syst Appl* 2006;31(3):495–503.
- [8] Mercorelli P. A denoising procedure using wavelet packets for instantaneous detection of pantograph oscillations. *Mech Syst Signal Process* 2013;35(1–2):137–49.
- [9] Tinati M, Mozaffary B. A wavelet packets approach to electrocardiograph baseline drift cancellation. *Int J Biomed Imag* 2006:1–9.
- [10] Peng Z. Application of the wavelet transform in machine condition monitoring and fault diagnostics: a review with bibliography. *Mech Syst Signal Process* 2004;18:199–221.
- [11] Lou X, Loparo K. Bearing fault diagnosis based on wavelet transform and fuzzy inference. *Mech Syst Signal Process* 2004;1077–95.
- [12] Wang W, McFaden P. Application of wavelets to gearbox vibration signals for fault detection. *J Sound Vib* 1996;192:927–39.
- [13] Gentile A, Messina A. On the continuous wavelet transforms applied to discrete vibrational data for detecting open cracks in damaged beams. *J Solid Struct* 2003;40:295–315.
- [14] Douka E, Loutridis S, Trochidis A. Crack identification in beams using wavelet analysis. *Int J Solids Struct* 2003;40:3557–69.
- [15] Herzog M, Marwala T, Heyns P. Machine and component residual life estimation through the application of neural networks. *Reliab Eng Syst Saf* 2009;94:479–89.
- [16] Fink O, Zio E, Weidmann U. Predicting component reliability and level of degradation with complex-valued neural networks. *Reliab Eng Syst Saf* 2014;121:198–206.
- [17] Santosh T, Srivastava A, Rao VS, Ghosh A, Kushwaha H. Diagnostic system for identification of accident scenarios in nuclear power plants using artificial neural networks. *Reliab Eng Syst Saf* 2009;94:759–62.
- [18] Martínez-Martínez S, Messai N, Jeannot J, Nuzillard D. Two neural network based strategies for the detection of a total instantaneous blockage of a sodium-cooled fast reactor. *Reliab Eng Syst Saf* 2015;137:50–7.
- [19] Babu T, Sekhar A. Shaft crack identification using artificial neural networks and wavelet transform data of a transient rotor. *Adv Vib Eng* 2010;9(3):207–14.
- [20] Srinivas H, Srinivasan K, Umesh K. Role of an artificial neural network and a wavelet transform for condition monitoring of the combined faults of unbalance and cracked rotors. *Int J Acoust Vib* 2010;15(3):121–7.
- [21] Dai H, Zhang B, Wang W. A multiwavelet support vector regression method for efficient reliability assessment. *Reliab Eng Syst Saf* 2015;136:132–9.
- [22] Kim K, Zuo M. Two fault classification methods for large systems when available data are limited. *Reliab Eng Syst Saf* 2007;92(5):585–92.
- [23] Bachschmid N, Penacci P. Editorial. Crack effects in rotordynamics. *Mech Syst Signal Process* 2008;22:761–2.
- [24] Han Q, Zhao J, Chu F. Dynamics analysis of a geared rotor system considering a slant crack on the shaft. *J Sound Vib* 2012;331:5803–23.
- [25] Han Q, Chu F. Parametric instability of a rotor-bearing system with two breathing transverse cracks. *Eur. J. Mech. A/Solids* 2012;36:180–90.
- [26] Han Q, Chu F. Parametric instability of a Jeffcott rotor with rotationally asymmetric inertia and transverse crack. *Nonlinear Dyn* 2013;73(1–2):827–42.
- [27] Castejón C, García-Prada J, Gómez M, Meneses J. Automatic detection of cracked rotors combining multiresolution analysis and artificial neural networks. *J Vib Control*, <http://dx.doi.org/10.1177/1077546313518816>.
- [28] Castejón C, Gómez M, García-Prada J, nez AO, Rubio H. Automatic selection of the wpt decomposition level for condition monitoring of rotor elements based on the sensitivity analysis of the wavelet energy. *Int J Acoust Vib* 2015;20(2):95–100.
- [29] Mallat S. A wavelet tour of signal processing. Academic Press; 1998.
- [30] Jensen A, la Cour-Harbo A. Ripples in mathematics. Springer; 2000.
- [31] Dai H, Zhang B, Wang W. A new evolutionary system for evolving artificial neural networks. *IEEE Trans Neural Netw* 1997;8:694–713.
- [32] Dai H, Zhang B, Wang W. A multiwavelet support vector regression method for efficient reliability assessment. *Reliab Eng Syst Saf* 2012;364:012023.
- [33] Lara O, Castejón C, García-Prada J. Bearing fault diagnosis based on neural network classification and wavelet transform. *WSEAS Trans Signal Process* 2006;2(10):1371–8.
- [34] Gómez M, Castejón C, García-Prada J. Incipient fault detection in bearings through the use of WPT energy and neural networks. In: *Advances in condition monitoring of machinery in non-stationary operations. Lecture notes in mechanical engineering*; 2014. p. 63–72.
- [35] Gómez M, Castejón C, Barber R, Rubio H, García-Prada J. Btool: a friendly teaching tool to acquire and process vibration signals. In: *Proceedings of the 14th IFTOMM world congress, Taipei, Taiwan*; 2015. <http://dx.doi.org/10.6567/IFTOMM.14TH.WC.OS5.001>.
- [36] Gómez M, Castejón C, García-Prada J. Crack detection in rotating shafts based on the 3x energy. *Mech Mach Theory* 2016;96:94–106.
- [37] Gómez M, Castejón C, García-Prada J. Energy analysis distribution regarding the crack size in a rotating shaft. In: *Proceedings of the 14th IFTOMM world congress, Taipei, Taiwan*; 2015. <http://dx.doi.org/10.6567/IFTOMM.14TH.WC.OS14.010>.
- [38] Chow M. Methodologies of using neural network and fuzzy-logic technologies for motor incipient fault detection. World Scientific; 1997.
- [39] Bachschmid N, Penacci P, Tanzi E. Some remarks on breathing mechanism, on non-linear effects and on slant and helicoidal cracks. *Mech Syst Signal Process* 2012;22:879–904.